

An Efficient Image Denoising using Moore Neighborhood Based Mirrored CA and IRNPR

S. Natheldha Mary Navina

Abstract— This paper confronts a novel approach for noisy pixel detection and restoration of gray scale image using mirrored cellular automata (CA). The proposed approach removes salt and pepper noise from a corrupted image. The proposed method allows extension of window size dynamically during high noise densities. The proposed method uses mirrored CA based on Moore neighborhood (8-neighborhood cell). This image denoising method is analyzed with several existing image denoising techniques such as, Median filter, Switch Median (SM) filter, Directional-Weighted-Median (DWM) filter, Modified DWM (MDWM), Fuzzy Cellular Automata (FCA), Modified Decision Based Unsymmetric Trimmed Median Filter (MDBUTMF), and Contra Harmonic Mean (CHM) filter. Three sample images (Lena, Boat, and Mandrill) of two different resolutions (512 x 512) and (256 x 256) are taken for the performance analysis. The mirrored CA is analyzed against Peak Signal-to-Noise Ratio (PSNR), Mean Squared Error (MSE), and Structural SIMilarity (SSIM). It is observed that mirrored CA performs better than the other existing methodologies in terms of PSNR.

Index Terms— Cellular Automata (CA), Mirrored CA, Mean Squared Error (MSE), Peak Signal-to-Noise Ratio (PSNR), and Structural SIMilarity (SSIM).

I. INTRODUCTION

Denoising is an important issue in image processing. Impulse noises are induced due to malfunctioning pixels in camera sensors or transmission in a noisy channel. Two common types of impulse noise are the random valued noise and the salt-and-pepper noise. For the images corrupted by salt-and-pepper noise, noisy pixels take only the maximum and the minimum values in the dynamic range. These noises will reduce the quality of images and damage the expression of information for images effectively. Image filtering can effectively reduce the noise in the image. The goal of impulse noise removal is to suppress the noise to preserve the integrity of edge and detail information. There are many works on the restoration of images corrupted by impulse noise. A good and efficient noise removal technique should remove maximum noise as well as it should retain the important feature as much as possible. The usual methods of image filtering in general are spatial filtering and frequency domain filtering. There are many filtering methods available to denoise the image. Earlier techniques find the neighboring extreme “noisy” pixel to be filtered out. Regrettably, the extreme pixels that are considered noise may also contain the original details which may as well be removed during the smoothing process.

Manuscript received Nov15, 2015.

S. Natheldha Mary Navina, Department of IT, SRIT, Coimbatore, India

An efficient denoising method is proposed using mirrored CA based on Moore neighborhood (8-neighborhood cell), Iterative Refined Noisy Pixel Restoration (IRNPR) with mirrored CA. This image denoising method is analyzed with several existing image denoising techniques such as, Median filter, Switch Median (SM) filter, Directional Weighted Median (DWM) filter, Modified DWM (MDWM), Fuzzy Cellular Automata (FCA), Modified Decision Based Unsymmetric Trimmed Median Filter (MDBUTMF), and Contra Harmonic Mean (CHM) filter. Three sample images (Lena, Boat, and Mandrill) of two different resolutions (512 x 512) and (256 x 256) are taken for the performance analysis. IRNPR-mirrored CA is analyzed against Peak Signal-to-Noise Ratio (PSNR), Mean Squared Error (MSE), and Structural SIMilarity (SSIM). It is observed that proposed method performs better than the other existing methodologies in terms of PSNR.

The rest of this paper is organized as below: Works that are related to the denoising of images are presented in Section II. The working and description of the proposed technique for the noise pixel detection and restoring of grey scale images are given elaborately in Section III. Efficiency and performance of the proposed method are analyzed through experimenting in the Section IV. Finally, Section V concludes with an idea to enhance the denoising technique in the future.

II. RELATED WORK

Toh and Isa [1] proposed a novel two-stage noise adaptive fuzzy switching median (NAFSM) filter for detection and removal of salt-and-pepper noise. First, the detection stage will utilize the histogram of the corrupted image to identify noise pixels. These detected “noise pixels” will then be subjected to the second stage of the filtering action, while “noise-free pixels” are retained and left unprocessed. Then, the NAFSM filtering mechanism applies fuzzy reasoning to handle uncertainty present in the extracted local information as introduced by noise. *Dharmarajan and Kannan* [2] proposed an algorithm for the hypergraph (HG) representation of an image, subsequent detection of Salt and Pepper (SP) noise in the image and finally the restoration of the image from this noise. Hyperedges themselves are determined by two Image Neighborhood Hypergraph (INHG) parameters, with the concepts of 8-bit neighborhood and INHG of a graph being central. The images carried for experimental analyses are subject to the Contra Harmonic Mean (CHM) filter for SP noise removal. *Protter and Elad*

[3] have utilized redundant and sparse representations for removing noise from the image. An algorithm named K-SVD was used to train a sparsified dictionary for the images that were corrupted. Here, the scholars generalized the above mentioned algorithm through the following ways (i) number of iterations were reduced for propagating the dictionary from one frame to another or next frame and (ii) patches were averaged in both temporal and spatial neighboring locations. These mentioned ways were used to have a considerable benefit in complexity and denoising performance. A special technique named support vector regression (SVR) was applied by the researchers of [4] in order to remove noise from an image. The support vector values and their weights were computed after the noisy images were trained with a ground-truth. These computed values were used to remove the random noise present in an image at various levels on a pixel-by-pixel basis. This is an example-based approach because it has used SVs for noise removal. The experimental result analysis presented in this article showed that the SVR based denoising method performs better than the Besov ball projection technique on the image that was non-natural in terms of both PSNR and visual inspection.

Academicians of the article [5] have used PCA along with local pixel grouping (LPG) for noise removal. With the aim to preserve the local structures, a vector variable was modeled from a pixel and their nearest neighbor. Their samples for training were elected from the local window through block matching based LPG. This method ensures that only similar content and sample blocks were used for the estimation of PCA transformation. For better performance, LPG-PCA method was iterated. Analysis result given in the paper expressed that the LPG-PCA method outperforms the state-of-the-art noise removal algorithms. Another technique was proposed in [6] for removal of random noise. This method used Nonlocal means algorithm for efficient noise removal and the results of the experiment showed that NL-means based algorithm performed well than the state-of-the-art denoising algorithm. *Changhong, et al.* [7] proposes a novel improved median filter algorithm for the images highly corrupted with salt-and-pepper noise. Initially, all the pixels are classified based on the local statistic information into signal pixels and noisy pixels by using the Max-Min noise detector. The noisy pixels are distinguished into three classes, such as low, moderate, and high-density noises. Eventually the weighted 8-neighborhood similarity function filter, the 5×5 median filter and the 4-neighborhood mean filter are adopted to remove the noises. The paper [8] describes the diligence of cellular automata (CA) for several image processing tasks such as denoising and feature detection. The current work concentrates on intensity images. The increased number of cell states (i.e. pixel intensities) leads to a vast increment in the number of potential rules. Therefore, a reduced intensity representation was used, leading to a three state cellular automata that was more practical. In accession, a modified sequential floating forward search mechanism was formulated in order to speed up the choice of good rule sets in the CA training stage. In paper [9] a new method was proposed to eliminate noise and to detect image edges through the function of fuzzy cellular automata as in [10]. In this method, eight specific contiguous states are

considered for each pixel and sixteen numbers are derived from these states. Such numbers are used as input for the fuzzy membership function. The fuzzy rule base was constructed in such a way as to correctly recognize the state of each pixel.

A Modified Decision Based Unsymmetrical Trimmed Median Filter (MDBUTMF) combined with Fuzzy Noise Reduction Method (FNRM) was proposed [11] for the restoration of color images that are highly corrupted by salt and pepper noise. This filter substitutes the noisy pixel by trimmed median value when the elements with 0's and 255's values are present. The partial noise removed images are further processed by FNRM to obtain a fully noise removed image. An improved version of the directional weighted median (DWM) filter was proposed in paper [12]. This method can significantly improve the performance of the directional-weighted-median filter as it includes additional directions (12 directions) for edge detection, whereas the DWM filter only employs four directions. These additional directions amend the accuracy of edge detection.

Esakkirajan, et al. [13] removed the high density salt and pepper noise in gray scale and color images using a modified decision based unsymmetric trimmed median filter. This algorithm exchanges the noisy pixel with the trimmed median value, when all the pixel values in the selected window are 0's and 255's. The noise pixel was substituted by the mean value of all the elements in the specified window. *Gorsevski, et al.* [14] detected grain boundaries in deformed rocks by a cellular automata scheme. Two-dimensional CA was applied to the extraction of thin sections from deformed rocks and grain boundary detection. The extracted boundaries contain features like orientation, shape, and spatial distribution, formed from a CA Moore's environment-based rules methodology. The Moore's environment consists of a 3×3 matrix of varying the states by differentiating between a middle pixel and its neighbors. These rules estimated the future state of each cell while the number of repetitions to simulate boundary detection was user-specified. The output at each round gives various detection conditions of grain boundaries. *Kumar and Sahoo* [15] proposed a novel technique for edge detection utilizing CA.

Chhabria and Shende [16] designed a CA image extraction algorithm for head and hand gestures recognition. This real time vision system can be applied in an interactive multimedia environment. It consists of image capture, image extraction, pattern connection, and command estimation. The gestures are linked to the pre-stored database of gestures. Then, the hardware movement was performed as per the linked gestures on quad-directions. This movement can also be controlled using voice commands. The cellular automata consist of a multi-dimensional array/grid of cells. These cells can occupy any of the finite number of possible states. The states of the cells are simultaneously updated according to a state transition function. *Aydogan* [17] formulated a Cellular Neural Network (CNN) based edge detection of 2D data. This CNN model was used for the detection of the image body and edges. A stochastic image processing algorithm was proposed based on the immediate neighborhood link of the cells. This method was used for edge detection and image enhancement. CNN was applied to field and synthetic data produced for

edge detection of thin surface geological entities that shield each other in different depths and dimensions. An evolutionary edge detector was proposed using varying rule CA by *Sato and Kanoh* [18]. The learning algorithm used here was gene expression programming, where the transition rule was encoded as the expression by the chromosome. Training CA was generated by Canny edge detector and two objective functions were calculated. The objective functions were optimized by a multi-objective evolutionary algorithm.

Qadir, et al. [19] proposed a novel image noise filtering algorithm based on CA. This method can also remove the impulsive noise from the noisy images. Non-uniform CA rules were designed to remove the noise from general and medical images. *Hsu, et al.* [20] developed an algorithm for salt and pepper noise reduction technique using CA. The software programming model known as CAID (Cellular Automata Image Denoising) toolkit was developed using MATLAB ®.

The properties about impulse or salt and pepper noise were discussed by *Selvapeter and Hordijk* [21]. In impulse noise, only a random portion of image pixels are corrupted. These noisy pixels either take very large value (gray scale value 255) as a positive impulse or very small value 0 as negative impulse. Fixed value boundary conditions are applied in the cellular automata filter in salt and pepper noise removal, i.e., update rule is applied only to the non-boundary cells. The majority CA update rule used to remove the impulse noise was discussed in the paper. The noise propagation resulted from the deterministic CA rule is solved by using a random rule for breaking majority ties. A CA model for removing salt and pepper noise and uniform noise was proposed by *Dalhoun, et al.* [22]. The proposed CA model initially checks the type of noise by evaluating the histogram of the noisy image. The CA transition rule which is used to remove the salt and pepper noise was discussed in the paper. The techniques for training CAs to execute fairly standard image processing tasks to a high level of performance for proposed by *Rosin* [23]. In CA, the fixed value boundary conditions are applied in which transition rules are implemented only to non-boundary cells. The rule set is tested at each pixel to verify if any of its rules agrees the pixel neighborhood pattern. The paper describes that the process of applying the rules are continued until the number of iterations has reached a preset maximum.

III. IMAGE DENOISING USING MIRRORED CA

This section describes the image denoising technique using IRNPR-mirrored CA. First, the overview of the noise filtering method is briefed with the architecture. Then, the IRNPR-mirrored CA for enhanced image denoising is discussed.

A. CA and its characteristics

In the salt and pepper noise, the corrupted pixel takes one of the two different values: black or white. The median filter is used to remove unwanted noise and increase image quality. CA consists of interconnected cells, each of which has an automaton. An automaton which is a simple machine used to execute simple calculations has a state changing with time

based on the neighboring cell's states. The CA model transition rule decides the neighborhood relationship between the automata. The state of automaton at time (t) depends on the state of neighbor cells at time (t-1).

There are four classes to classify all possible behavior in CA. In class 3, almost all initial configurations relax after a transient period to apparently unpredictable space time behavior. Most of the uniform cellular automata are class 3.

B. Application of CA in image processing

Uniform cellular automata rules are built to remove impulse noise from binary and gray scale images. A random CA rule is used to minimize noise propagation present in deterministic CA filters. A Moore neighborhood (the eight neighboring cells surrounding a cell) is considered. A 2-D CA with a simple update rule is applied as effective impulse noise filter in digital images. CA implements fixed value boundary conditions where the update rule is applied only to non-boundary cells. The initial CA lattice configuration is the image corrupted by an impulse image.

The majority CA update rule states that if the center pixel gray level is 0 or 255, then the majority gray level in the local neighborhood is used to replace the center pixel's value. The deterministic or random CA majority rule is used when there is no majority gray level in the local neighborhood. In the random majority rule, the gray value of randomly chosen pixel in the neighborhood replaces the center pixel. In the deterministic majority rule, the fixed gray level in the neighborhood replaces the center pixel. The noise propagation resulted from the deterministic CA rule is solved by random rule. A random CA performs better than the deterministic CA for gray level images. CA transition rule is used in the removal of salt and pepper noise. This rule checks if the current pixel is corrupted. In case of occurrence of noise, if all neighbors are noisy, the current pixel is replaced by the average of neighbors. If all neighbors are not noisy, then their median value replaces the current automation state. The fixed boundary problem can be solved by mirrored CA.

C. Architecture of noise filtering

Initially, a test image is processed to detect the presence of impulse noise. Any pixel of the image is selected and checked whether it is noise free or noisy. This is done by checking whether the selected pixel value is maximum or minimum (0 or 255). If the value is either 0 or 255 then the pixel is noisy and processed by Iterative Refining technique. Else if the values are not 0 or 255, the pixel is noise free and left unchanged.

$$X_{i,j} = \begin{cases} 0 \text{ or } 255, & \text{noisy pixel} \\ \text{Otherwise,} & \text{noise free} \end{cases} \quad (1)$$

Where

$X_{i,j}$ = Intensity value of pixel at location (i, j)

$$X_{i,j} = \begin{cases} \text{noisy,} & \text{proceed IRNPR with CA} \\ \text{noise free,} & \text{no change} \end{cases} \quad (2)$$

Further, a 3×3 window centered at (i, j) is applied to the noisy pixel. To replace this noisy pixel, the neighbor pixels of this pixel are considered using IRNPR-mirrored CA, and then checked whether all the neighboring pixels are noisy or not.

CA with buffering system is used in the proposed method. i.e., while calculating the value of selected pixel at time t, the value of neighboring pixels at time (t-1) stored in the buffer is utilized. CA can be defined as (I, N, V, F).

I is a cellular space formed by a two dimensional array of m x n cells.

$$I = \{(a, b), 1 \leq a \leq m, 1 \leq b \leq n\}$$

N – Type of neighborhood (Moore neighborhood)

V – Set of neighborhood pixel value

F – Transition function

If all the neighboring pixels are noisy i.e. they have values either 0 or 255 as shown in (3), then they are considered as noisy pixel and the window is extended to 5x5.

$$\begin{bmatrix} 255 & 0 & 255 \\ 0 & < 255 > & 255 \\ 0 & 255 & 0 \end{bmatrix}$$

If at least some of the pixels are not noisy, then the median of the neighbor pixels are calculated by excluding the noisy pixels (0 or 255). The selected pixel is replaced with this median value. Then the process is moved to next pixel.

Consider a 3x3 window as in figure 2. Here X(i, j) is the selected pixel and other pixels are neighbors of X(i, j).

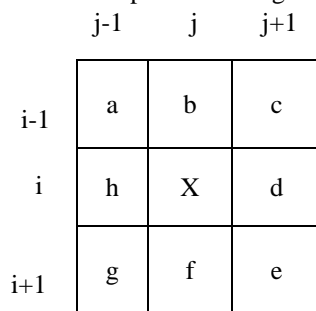


Fig 2. 3x3 window.

$$P = \begin{cases} \forall p(i, j) \text{ are noisy, Extend to } W_{5 \times 5} \\ \text{Otherwise, } \mu \text{ excluding } 0 \text{ and } 255 \end{cases} \quad (4)$$

Where P = contains all 8 neighbor pixels of X(i, j)

$$X(i, j) = \{\mu \text{ excluding extreme}\} \quad (5)$$

If the noise persists in 5x5 window also, then the window is extended to 7x7. If the pixels are not noisy find the median value of remaining pixels of 5x5 window and restore the value to X(i, j) as in equation 5. If all the neighboring pixels are noisy in 7x7 window, the mean value of neighbors is calculated else if some of the neighboring pixels are not noisy in 7x7 window, then the median value of remaining pixels excluding noisy pixels is calculated. Then the selected pixel is replaced with the calculated value.

$$X(i, j) = \begin{cases} \forall p(i, j) \text{ are noisy, } \text{Mean}(\forall p(i, j)) \\ \text{otherwise, } \mu \text{ excluding } 0 \text{ and } 255 \end{cases} \quad (6)$$

$$i_n = \begin{cases} \text{noisy } p(i, j), & \text{repeat IRNPR} \\ \forall p(i, j) \text{ noise free,} & i_{nf} \end{cases} \quad (7)$$

Finally, after employing these processes for every pixel in the image, the restored image is obtained. The quality of the image is analyzed using Mean square error. If the MSE of the denoised image is lower than the MSE of previous generation cellular automata, the image is noise free. Else the image consists of noise. When a low MSE restored image is obtained, that forms the final denoised noise-free image.

$$i_{nf} = \begin{cases} \text{Low MSE, } i_{nf} \\ \text{High MSE, } i_n \end{cases} \quad (8)$$

IV. PERFORMANCE ANALYSIS

(3) The proposed image denoising method is analyzed for four different gray scale images of two different resolutions each. The images are Lena (512 x 512), (256 x 256), Boat (512 x 512), (256 x 256), and Mandrill (512 x 512), (256 x 256). A sample of original Lena, Boat, and Mandrill images are given in Fig. 2.

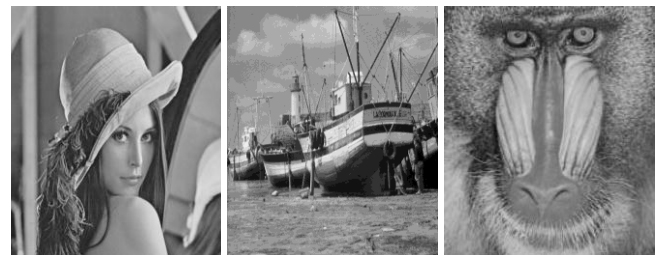


Fig. 3. Sample images (Left to Right): Lena, Boat, and Mandrill.

A. Results for 10% salt & pepper noise



Fig 4. Image Lena (Left to Right): Input noisy image and denoised image (without CA)



Fig. 5. Image Lena (Left to Right): Noisy Image and denoised image (with CA)

TABLE I
MSE, PSNR and SSIM values for 10% salt and pepper noise in Lena image

	MSE	PSNR	SSIM
Noisy Image	1.8605e+03	15.4344	0.4019
Without CA	27.2664	33.7745	0.9784
With CA	3.1119	43.2006	0.9977

B. Results for 90% salt & pepper noise

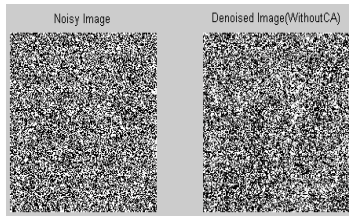


Fig. 6. Image Lena (Left to Right): Noisy input image and denoised image (without CA)

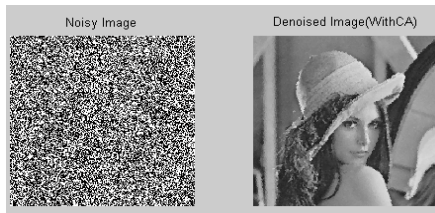


Fig. 7. Image Lena (Left to Right): Noisy image and denoised image (with CA).

TABLE II

MSE, PSNR and SSIM values for 90% salt and pepper noise in Lena image

	MSE	PSNR	SSIM
Noisy image	1.6701e+04	5.9034	0.0273
Without CA	1.4083e+04	6.6437	0.0247
With CA	172.8126	25.7550	0.8682

C. For Boat image – 10% noise

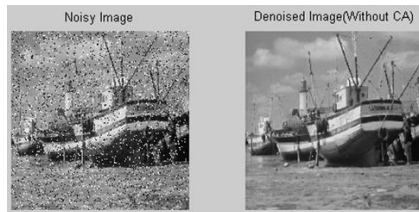


Fig. 8. Image Boat (Left to Right): Noisy input image and denoised image (without CA)

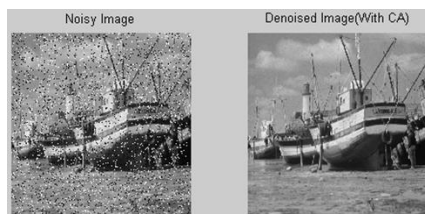


Fig. 9. Image Boat (Left to Right): Noisy image and denoised image (with CA)

TABLE III

MSE, PSNR and SSIM values for 10% noise in boat image

	MSE	PSNR	SSIM
Noisy Image	1.8589e+03	15.4382	0.4576
Without CA	69.4081	29.7167	0.9581
With CA	8.0039	39.0978	0.9952

D. For boat – 90% noise

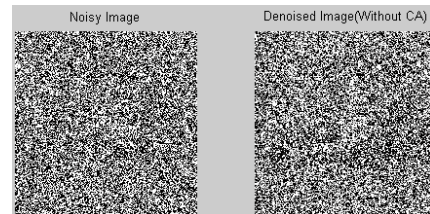


Fig. 10. Image Boat (Left to Right): Noisy input image and denoised image (without CA)

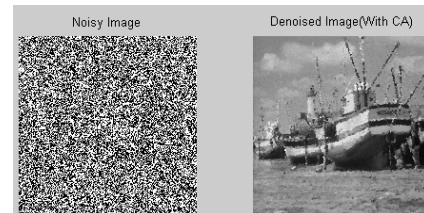


Fig. 11. Image Boat (Left to Right): Noisy image and denoised image (with CA)

TABLE IV

MSE, PSNR and SSIM values for 90% noise in boat image

	MSE	PSNR	SSIM
Noisy Image	1.6588e+04	5.9329	0.0317
Without CA	1.4028e+04	6.6607	0.0284
With CA	304.2348	23.2987	0.7909

E. For Mandrill – 10% noise

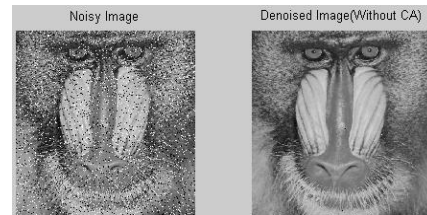


Fig. 12. Image Mandrill (Left to Right): Noisy input image and denoised image (without CA)

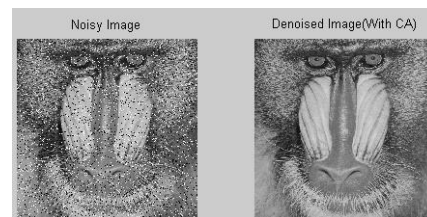


Fig. 13. Image Mandrill (Left to Right): Noisy image and denoised image (with CA)

TABLE V

MSE, PSNR and SSIM values for 10% noise in mandrill image

	MSE	PSNR	SSIM
Noisy Image	1.8241e+03	15.5203	0.5638
Without CA	283.4876	23.6055	0.9019
With CA	38.7515	32.2479	0.9898

F. For Mandrill – 90% noise

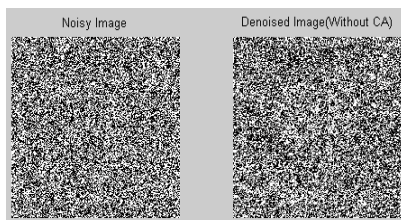


Fig. 14. Image Mandrill (Left to Right): Noisy input image and denoised image (without CA)

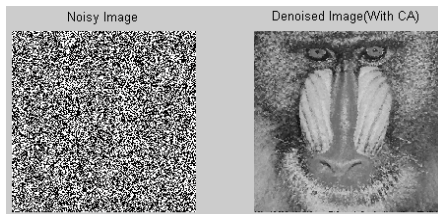


Fig. 15. Image Mandrill (Left to Right): Noisy image and denoised image (with CA)

TABLE VI

MSE, PSNR and SSIM values for 90% noise in mandrill image

	MSE	PSNR	SSIM
Noisy Image	1.6288e+04	6.0122	0.0345
Without CA	1.3893e+04	6.7028	0.0276
With CA	744.1779	19.4140	0.6249

G. Comparison with existing methods

The images are analyzed in terms of Peak Signal-to-Noise Ratio (PSNR) [25], Mean Squared Error (MSE) [25], and Structural Similarity (SSIM) [26].

$$MSE = \frac{\sum_m \sum_n (f(m,n) - \hat{f}(m,n))^2}{x \times y} \quad (9)$$

$$PSNR \text{ (dB)} = 10 \log_{10} (255^2 / MSE) \quad (10)$$

$$SSIM = \frac{(2\mu_a\mu_b + c_1)(2\sigma_{ab} + c_2)}{(\mu_a^2 + \mu_b^2 + c_1)(\sigma_a^2 + \sigma_b^2 + c_2)} \quad (11)$$

In (9), (m, n) represents the current pixel location. In (11), two non-negative image signals a and b are aligned with one another for the measurement of SSIM [26]. The following notations are used in (11):

- μ_a is the average of a .
- μ_b is the average of b .
- σ_a^2 is the variance of a .
- σ_b^2 is the variance of b .
- σ_{ab} is the covariance of ab .
- C_1 and C_2 are two constants to avoid instability [26].

The existing image denoising methods taken for the analysis are Median filter [27], Switch Median (SM) filter [1], Directional-Weighted-Median (DWM) filter [12], Modified DWM (MDWM) [4], Fuzzy Cellular Automata (FCA) [10], Modified Decision Based Unsymmetric Trimmed Median Filter (MDBUTMF) [19], and Contra Harmonic Mean (CHM) filter [10].

TABLE VII

PSNR (dB) for Lena (512×512) image for different window sizes, various noise densities and IRNPR-mirrored CA

Noise Density	3×3	3×3 or 5×5	Refined 3×3 or 5×5	Iterative refined 3×3 or 5×5 or 7×7
10	42.97	42.91	42.9944	43.0698
20	39.20	39.14	39.1135	39.2165
30	36.64	36.61	36.7338	36.6313
40	33.87	34.56	34.9466	34.8904
50	29.98	32.63	33.3527	33.1090
60	24.49	29.14	31.6570	31.8089
70	19.36	23.33	29.9900	30.1723
80	14.26	16.66	26.0760	28.4337
90	9.76	10.72	16.8664	25.9115

PSNR is analyzed for Lena (512×512) image for different window sizes, various noise densities and IRNPR-mirrored CA. The comparative analyses are given in TABLE VII.

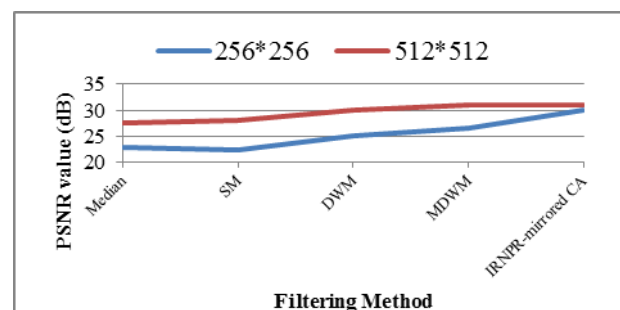
PSNR is analyzed for Lena (512×512) image for different noise densities using IRNPR-mirrored CA and other existing methods. The comparative analysis is given in TABLE VIII.

TABLE VIII

PSNR for Lena image (512×512) using IRNPR-mirrored CA and other existing methods

Noise Density	SM	DWM	MDWM	FCA	CHM	IRNPR-mirrored CA
10	36.12	40.78	41.45	35	37.31	43.06
20	33.42	37.02	38.22	33.50	34.59	39.21
30	31.36	34.63	35.97	32.70	32.99	36.63
40	29.88	32.51	34.07	31.20	33.01	34.89
50	28.54	30.23	32.69	29.20	29.53	33.10
60	26.76	27.69	31.21	27.80	27.20	31.80
70	24.47	25.23	29.72	26.50	26.45	30.17
80	19.52	21	27.94	23.70	22.56	28.43
90	8.80	15.45	25.50	18.37	19.57	25.91

PSNR is analyzed for two resolutions of the Lena image (512×512), and $(256, 256)$, using IRNPR-mirrored CA and other existing methods. The comparative analysis is given in Fig. 17

Fig. 17. Graphical analysis of PSNR for 2 two resolutions of Lena image (512×512), and $(256, 256)$, using IRNPR-mirrored CA and other existing methods.

PSNR is analyzed for Lena image (512×512) using IRNPR-mirrored CA and other existing methods. The comparative analysis is given in Fig. 18.

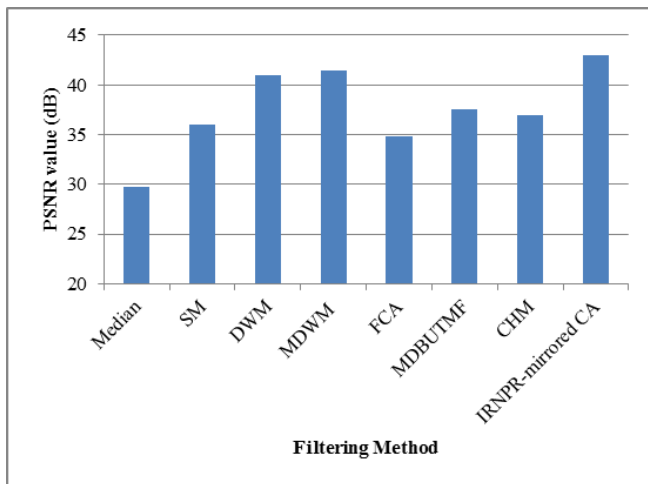


Fig. 18. Graphical analysis of PSNR for Lena image (512×512) using IRNPR-mirrored CA and other existing methods.

PSNR is analyzed for Lena image (256×256) using IRNPR-mirrored CA and other existing methods. The comparative analyses are given in Fig. 19.

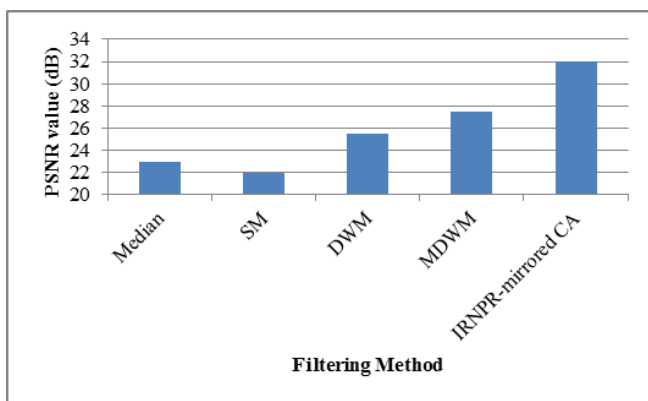


Fig. 19. Graphical analysis of PSNR for Lena (256×256) image using IRNPR-mirrored CA and other existing methods.

PSNR, MSE, and SSIM are analyzed for Lena (512×512) image for different noise densities using IRNPR-mirrored CA. The comparative analysis is given in TABLE X

TABLE X
PSNR, MSE, SSIM for Lena (512×512) image for different noise densities using IRNPR-mirrored CA

Noise Density	PSNR(dB)	MSE	SSIM
10	43.06	3.20	0.99
20	39.21	7.78	0.99
30	36.63	14.12	0.99
40	34.89	21.08	0.98
50	33.10	31.78	0.97
60	31.80	42.87	0.96
70	30.17	62.49	0.95
80	28.43	93.26	0.92
90	25.91	166.69	0.86

PSNR, MSE, and SSIM are analyzed for Lena (256×256) image for different noise densities using IRNPR-mirrored CA. The comparative analysis is given in TABLE XI

TABLE XI

PSNR, MSE, SSIM for Lena (256×256) image for different noise densities using IRNPR-mirrored CA.

Noise Density	PSNR(dB)	MSE	SSIM
10	41.26	4.8593	0.9930
20	37.23	12.2804	0.9833
30	34.73	21.8583	0.9712
40	32.83	33.8814	0.9567
50	31.16	49.7245	0.9387
60	29.71	69.4259	0.9171
70	28.17	98.8871	0.8861
80	26.30	152.2680	0.8341
90	23.73	274.8842	0.7436

V. CONCLUSION

An efficient denoising method is proposed using mirrored CA based on Moore neighborhood (8-neighborhood cell). This image denoising method is analyzed with several existing image denoising techniques such as, Median filter, Switch Median (SM) filter, Directional-Weighted-Median (DWM) filter, Modified DWM (MDWM), Fuzzy Cellular Automata (FCA), Modified Decision Based Unsymmetric Trimmed Median Filter (MDBUTMF), and Contra Harmonic Mean (CHM) filter. Three sample images (Lena, Boat, and Mandrill) of two different resolutions (512×512) and (256×256) are taken for the performance analysis. The mirrored CA is analyzed against Peak Signal-to-Noise Ratio (PSNR), Mean Squared Error (MSE), and Structural SIMilarity (SSIM). It is observed that mirrored CA performs better than the other existing methodologies in terms of PSNR. This mirrored CA based image denoising method can be expanded to higher resolution image processing with faster computing techniques like parallel computing.

REFERENCES

- [1] K. K. V. Toh and N. A. M. Isa, "Noise Adaptive Fuzzy Switching Median Filter for Salt-and-Pepper Noise Reduction," *Signal Processing Letters, IEEE*, vol. 17, pp. 281-284, 2010.
- [2] R. Dharmarajan and K. Kannan, "A hypergraph-based algorithm for image restoration from salt and pepper noise," *AEU - International Journal of Electronics and Communications*, vol. 64, pp. 1114-1122, 2010.
- [3] M. Protter and M. Elad, "Image Sequence Denoising via Sparse and Redundant Representations," *Image Processing, IEEE Transactions on*, vol. 18, pp. 27-35, 2009.
- [4] D. Li, "Support vector regression based image denoising," *Image and Vision Computing*, vol. 27, pp. 623-627, 2009.
- [5] L. Zhang, W. Dong, D. Zhang, and G. Shi, "Two-stage image denoising by principal component analysis with local pixel grouping," *Pattern Recognition*, vol. 43, pp. 1531-1549, 2010.
- [6] K. Lu, N. He, and L. Li, "Nonlocal Means-Based Denoising for Medical Images," *Computational and Mathematical Methods in Medicine*, vol. 2012, pp. 1-8, 2012.
- [7] W. Changhong, C. Taoyi, and Q. Zhenshen, "A novel improved median filter for salt-and-pepper noise from highly corrupted images," in *Systems and Control in Aeronautics and Astronautics (ISSCAA), 2010 3rd International Symposium on*, 2010, pp. 718-722.
- [8] P. L. Rosin, "Image processing using 3-state cellular automata," *Computer Vision and Image Understanding*, vol. 114, pp. 790-802, 2010.
- [9] K. Mirzaei, H. Motameni, and R. Enayatifar, "New method for edge detection and de noising via fuzzy cellular automata," *Int. J. Phy. Sci.*, vol. 6, pp. 3175-3180, 2011.

- [10] S. Sadeghi, A. Rezvanian, and E. Kamrani, "An efficient method for impulse noise reduction from images using fuzzy cellular automata," *AEU - International Journal of Electronics and Communications*, vol. 66, pp. 772-779, 2012.
- [11] T. Vimala, "Salt and pepper noise reduction using mdb utm filter with fuzzy based refinement," *International Journal of Management, IT and Engineering*, vol. 2, pp. 447-461, 2012.
- [12] C.-T. Lu and T.-C. Chou, "Denoising of salt-and-pepper noise corrupted image using modified directional-weighted-median filter," *Pattern Recognition Letters*, vol. 33, pp. 1287-1295, 2012.
- [13] Esakkirajan, S. Veerakumar, T. ; Subramanyam, A.N. ; PremChand, C.H.," Removal of High Density Salt and Pepper Noise Through Modified Decision Based Unsymmetric Trimmed Median Filter", *IEEE Signal Processing Letters*, Volume:18 Issue:5, pp. 287 - 290, 2011.
- [14] P. V. Gorsevski, C. M. Onasch, J. R. Farver, and X. Ye, "Detecting grain boundaries in deformed rocks using a cellular automata approach," *Computers & Geosciences*, vol. 42, pp. 136-142, 2012.
- [15] T. Kumar and G. Sahoo, "A Novel method of edge detection using cellular automata," *International Journal of Computer Applications*, vol. 9, pp. 38-44, 2010.
- [16] S. A. Chhabria and R. S. Shende, "Cellular Automata Image Extraction Algorithm for Gestures Recognition," *International Journal on Computer Science and Technology*, vol. 2, pp. 251-255, 2011.
- [17] D. Aydogan, "CNNEDGE POT: CNN based edge detection of 2D near surface potential field data," *Computers & Geosciences*, vol. 46, pp. 1-8, 2012.
- [18] S. Sato and H. Kanoh, "Evolutionary design of edge detector using rule-changing Cellular automata," in *Nature and Biologically Inspired Computing (NaBIC), 2010 Second World Congress on*, 2010, pp. 60-65.
- [19] F. Qadir, M. A. Peer, and K. A. Khan, "An effective image noise filtering algorithm using cellular automata," in *Computer Communication and Informatics (ICCCI), 2012 International Conference on*, 2012, pp. 1-5.
- [20] C.-Y. Hsu, T.-S. Tsui, S.-S. Yu, and K.-K. Tseng, "Salt and Pepper Noise Reduction by Cellular Automata," *International Journal of Applied Science and Engineering*, vol. 9, pp. 2-19, 2011.
- [21] P. J. Selvapeter and W. Hordijk, "Cellular automata for image noise filtering," in *Nature & Biologically Inspired Computing, 2009. NaBIC 2009. World Congress on*, 2009, pp. 193-197.
- [22] A. I. A. Dalhoum, I. Al-Dhamari, A. Ortega, and M. Alfonseca, "Enhanced Cellular Automata for Image Noise Removal," pp. 1-5.
- [23] P. L. Rosin, "Training Cellular Automata for Image Processing," *IEEE Transactions On Image Processing*, vol. VOL. 15, pp. 1-12, 2006.
- [25] S. Esakkirajan, T. Veerakumar, A. N. Subramanyam, and C. H. PremChand, "Removal of High Density Salt and Pepper Noise Through Modified Decision Based Unsymmetric Trimmed Median Filter," *Signal Processing Letters, IEEE*, vol. 18, pp. 287-290, 2011.
- [26] W. Zhou, A. C. Bovik, H. R. Sheikh, and E. P. Simoncelli, "Image quality assessment: from error visibility to structural similarity," *Image Processing, IEEE Transactions on*, vol. 13, pp. 600-612, 2004.
- [27] M.-H. Hsieh, F.-C. Cheng, M.-C. Shie, and S.-J. Ruan, "Fast and efficient median filter for removing 1–99% levels of salt-and-pepper noise in images," *Engineering Applications of Artificial Intelligence*, vol. 26, pp. 1333-1338, 2013.

S. Natheldha Mary Navina is working as an Assistant Professor in the department of Information Technology, Sri Ramakrishna Institute of Technology, Coimbatore. She did her BE degree in Tirunelveli and ME degree in Coimbatore. Her research area includes Image Denoising and Image Segmentation.